



OPEN

In vivo and in silico studies on the potential role of garden cress oil in attenuating methotrexate-induced inflammation and apoptosis in liver

Dalia M. Mabrouk¹, Radwa H. El-Akad², Ahmed H. Afifi², Hafiza A. Sharaf³,
Sonia L. El-Sharkawy³ & Aida I. El makawy¹✉

Methotrexate (MTX) has been used in high doses for cancer therapy and low doses for autoimmune diseases. It is proven that methotrexate-induced hepatotoxicity occurs even at relatively low doses. It is known that garden cress has anti-inflammatory, antioxidant, and hepatoprotective properties. This study investigates the potential alleviating effect of garden cress oil (GCO) against MTX-induced hepatotoxicity in rats. The chemical composition of GCO was assessed using GC/MS analysis. Liver damage was studied using hepatotoxicity biomarkers, molecular, and histological analysis. Also, the effects of GCO on TNF- α and caspase-3 proteins were evaluated through molecular docking studies. The results demonstrated that MTX caused liver damage, as seen by elevated levels of the liver enzymes ALT, AST, and ALP. Likewise, MTX showed clear signs of apoptosis, such as increased mRNA expression levels of BAX, Caspase-3, and P53, and increased liver inflammation indicated by higher levels of TNF- α expression. MTX exhibited significant liver damage, as demonstrated by histological examination. Treatment with GCO effectively alleviated the apoptotic effects of MTX, provided protection against inflammation, and restored histological alterations. GC/MS metabolite profiling of garden cress oil revealed the presence of several phytoconstituents, including tocopherols, erucic acid, sesamolin, linoleic acid, vaccenic acid, oleic acid, stearic acid, and palmitic acid, that showed strong binding affinities toward TNF- α and caspase-3 proteins in molecular docking studies, which could explain the anti-apoptotic and anti-inflammatory potential of GCO.

Keywords Methotrexate, Hepatotoxicity, Garden cress, In silico, Inflammation, Apoptosis

Drug-induced liver injury is a significant issue that limits the duration of medication therapy and undermines its positive effects. These effects could potentially result from modifications in distinct pathways that trigger an immediate toxic effect, the production of active metabolites, or an immune response. Consequently, over the last decade, researchers, government agencies, medical professionals, and pharmaceutical companies have all paid close attention to the rise in drug-induced liver damage. Over a thousand medications have been linked to liver injury, which can lead to inflammation, liver cell death, and severe liver failure¹.

Methotrexate (MTX) is one of the most effective and widely used drugs in the management of autoimmune diseases². Methotrexate is specified for a variety of medical conditions, including autoimmune rheumatic, psoriatic and juvenile idiopathic arthritis, inflammatory myopathies, sarcoidosis, rheumatic polymyalgia, arthritis related to secondary amyloidosis, and others. It is also used for other autoimmune conditions, such as Sjogren syndrome, inflammatory bowel disease, vasculitis, and some neoplasms^{3,4}. It is an antifolic acid medication derived from aminopterin that can inhibit DNA synthesis and repair^{5,6}. One potential mechanism for MTX-induced liver damage is the prolonged presence of MTX in cells due to hepatocytes storing and metabolizing it in its polyglutamated form^{7,8}. Disruption of the intestinal barrier function may lead to methotrexate-induced hepatotoxicity, allowing bacteria to translocate to the liver and cause damage. Furthermore, MTX has been shown to increase intestinal permeability, which is linked to elevated hepatic enzymes, fibrosis, cirrhosis, and hepatic inflammation⁹. Several studies have indicated that hepatotoxicity can result from an imbalance in the

¹Cell Biology Department, Biotechnology Research Institute, National Research Centre, P.O.12622, Giza, Egypt.

²Pharmacognosy Department, Pharmaceutical and Drug Industries Research Institute, National Research Centre, PO Box 12622, Cairo, Egypt. ³Pathology Department, Medical Research and Clinical Studies Institute, National Research Centre, P.O.12622, Giza, Egypt. ✉email: aelmakawy@yahoo.com

regulation of oxidative stress, inflammation, endothelial damage, and apoptosis^{2,10–14}. Additionally, MTX may be used in lower dosages as a disease-modifying anti-rheumatic drug for autoimmune diseases, but this use can still result in liver damage as a side effect¹⁵, indicating that MTX-induced hepatotoxicity may not be dose-dependent¹⁶.

Apoptosis is essential for maintaining tissue homeostasis in the body and occurs under the control of different genes in multicellular and unicellular organisms. The pro-apoptotic Bcl-associated X (BAX) protein and anti-apoptotic B-cell lymphoma 2 (Bcl-2) protein play significant roles in forming mitochondrial apoptotic channels. Caspase protease enzymes, including caspase-3 and 7, are also involved in various apoptotic pathways. The TP53 gene is one of the most widely studied genes in human cells due to its multifaceted functions and complex dynamics. P53 can induce apoptosis in a genetically unstable cell by interacting with many pro-apoptotic and anti-apoptotic factors^{17,18}. In addition, TNF α , mainly produced by activated macrophages during inflammation, has been implicated as an important pathogenic mediator in liver diseases¹⁹.

It has been reported that plant-based medicines are a source of biologically active ingredients and are important in global healthcare, including alternative, conventional, and preventative medicine²⁰. *Lepidium sativum* (LS) or Garden cress, a member of the Brassicaceae family, can be topically used to relieve rheumatism, inflammation, and sore muscles²¹. Additionally, it has hepatoprotective, anti-diarrheal, antioxidant, blood-purifying, hunger-stimulating, antispasmodic, and anticancer properties^{22,23}. It also possesses anti-diabetic, laxative, cholesterol-lowering, fracture-healing, pain-relieving, procoagulant, and diuretic properties. According to Emhofer et al.²⁴, it contains proteins, vitamins, carbohydrates, omega-3 fatty acids, iron, phytochemicals, and flavonoids. The liver-protective properties of garden cress seeds have come to light due to their ability to promote liver function and protect it from injury. Therefore, many studies are investigating the bioactive compounds in garden cress seeds and their impact on liver function²⁵. In conventional medicine, garden cress seed treat inflammatory conditions like diabetes mellitus, arthritis, and hepatitis²⁶. Abdulaziz et al.²⁷ found that garden cress strongly inhibits inflammation-progressing enzymes (COX1 and 2). Sayed et al.²⁸ indicated that *Lepidium sativum* (LS) can modulate the expression of inflammation markers such as IL-6, TNF- α , IL-4, and IL-10 in lipopolysaccharide-induced liver damage in mice.

The purpose of this study was to explore three main objectives: 1) to examine the potential impact of garden cress oil on reducing hepatotoxicity caused by low-dose methotrexate in rats, 2) to analyze the chemical composition of GCO, and 3) to predict the binding modes and affinities of the major metabolites against potential biological targets using molecular docking tools.

Results

Lipid content determination in GCO via GC/MS analysis

Total ion chromatograms of the analyzed unsaponifiable matter (unsap.) and FAME are shown in Fig. 1. The area percentage of identified compounds is presented in Table 1 and Table 2. Analysis of unsaponifiable matter revealed the identification of 67 metabolites constituting 89.5%; the majority of which are alkane hydrocarbons (80.26%) varying between branched and straight chain (Table 1). Herein, 36 alkane hydrocarbons were detected. Long chain unsaturated fatty alcohols docosenol (15.1%) and eicosenol (15.01%) were the major compounds in the analyzed sample (Table 1). Other detected compounds included alcohols, esters and aldehydes of saturated and unsaturated hydrocarbon chains varying from C-12 to C-31 (Table 1).

Other identified compounds belong to diverse phytochemical classes including 19 mono-/sesqui-/di- and tri-terpenes (4.75%), 2 phenyl propanoids (0.5%), 3 tocopherols (0.08%), 2 lignans (Sesamin (0.97%) and sesamolin (1.5%) and 6 sterols (1.59%) (Fig. 2). Carotane sesquiterpenes, carotol (1.1%) and daucol (0.05%), are reported herein for the first time as well as bisabolene (0.73%), cuparene (0.027%) and cupranene (0.011%). Conversely, 6 fatty acids were identified as methyl esters (92.02%) that included oleic (33.1%) and linoleic acids (30.9%) followed by erucic, vaccenic, palmitic and stearic acids (Table 2).

Molecular docking study

Molecular docking study was employed to assess the binding affinities and binding poses of the identified phytoconstituents in garden cress oil against the active sites of TNF- α (pdb: 7JRA) and Caspase-3 (pdb: 3GJQ) with the aim to predict the underlying mechanism of the hepatoprotective effect of garden cress oil against MTX-induced hepatotoxicity. Table 3 displays the binding energy of the top-scoring phytoconstituents against the two targets.

Validation of the docking protocol was assessed through redocking of the co-crystallized ligands against their corresponding proteins and calculating the RMSD value between the docked pose and the co-crystallized pose for both ligands. The validity of the docking parameters was donated by the excellent superposition and small RMSD value between docked and co-crystallized poses for both ligand (0.587 and 0.846 Å for TNF- α and Caspase-3, respectively).

Among the identified phytoconstituents, α , β and γ -tocopherols along with erucic acid and Sesamolin exhibited the highest binding affinities toward the TNF- α binding site with binding energies -9.55, -10.73, -9.52, -9.97 and -9.91 kcal/mol, respectively. Inspection of the best scoring pose of β -tocopherol in the active site of the TNF- α homotrimer revealed the formation of one conventional hydrogen bond between the phenolic hydroxyl group of β -tocopherol and Gly197 residue in chain B of TNF- α . Moreover, several hydrophobic interactions have also contributed to anchor the compound in the hydrophobic binding cavity (Fig. 3). On the other hand, the highest binding affinities to the Caspase-3 active site were observed by linoleic acid, vaccenic acid, oleic acid, stearic acid and palmitic acid as they achieved binding energies of -10.05, -7.48, -7.45, -6.93 and -6.89 kcal/mol, respectively. The best scoring pose of linoleic acid displayed its binding to the active site at the interface between p17 (chain A) and p12 (chain B) subunits of the caspase-3 heterodimer and the formation of three conventional hydrogen bonds by linoleic acid carboxylic group with the residues Arg64 (chain A), Gln161 (chain A) and

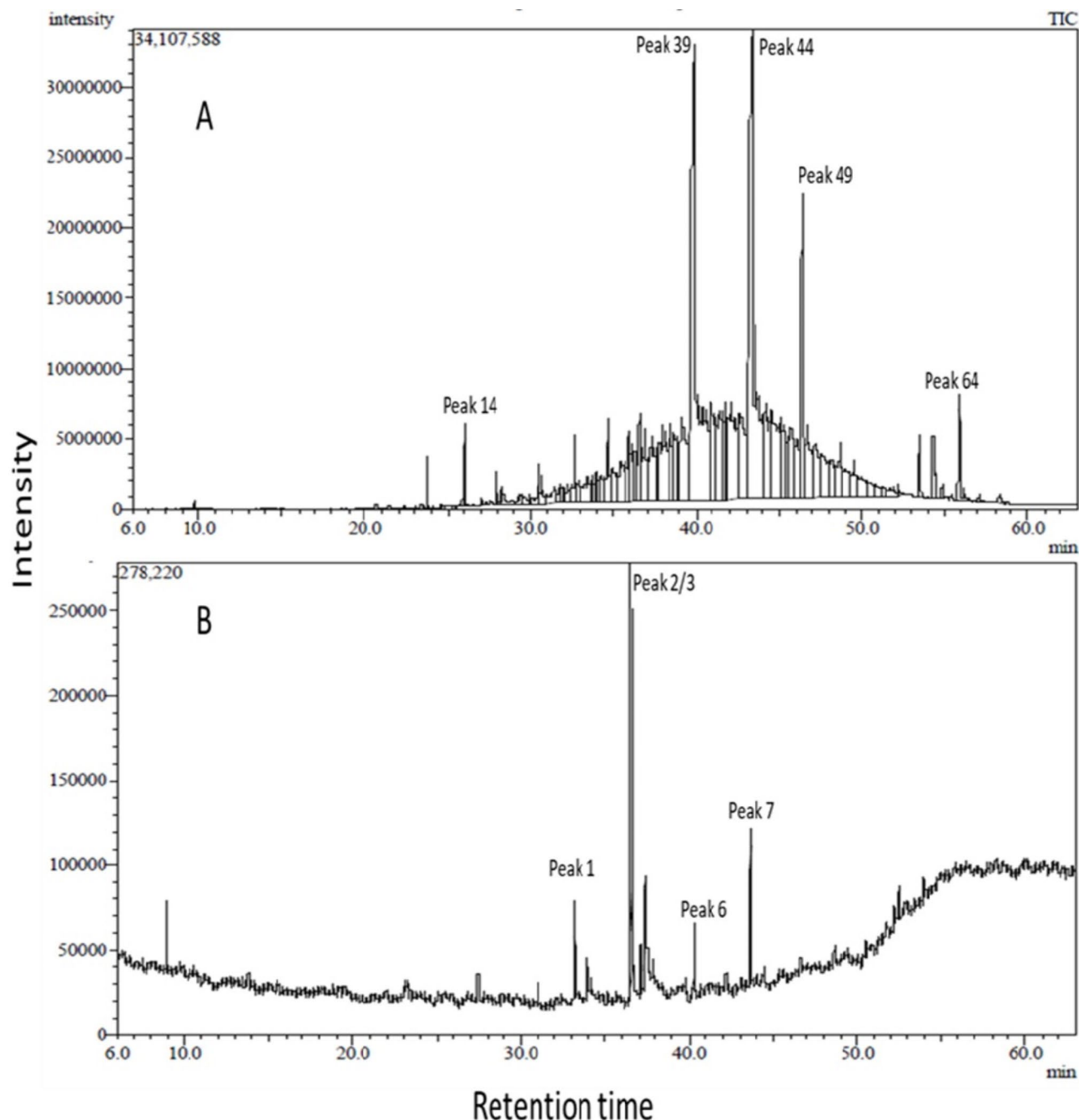


Fig. 1. Total ion chromatograms of unsaponifiable matter (A) and fatty acid methyl esters (B) detected in garden cress seed oil (*Lepidium sativum*) via GC/MS analyses. Peaks follow the numbering of identified compounds in Table 1 and Table 2.

Arg207 (chain B) in addition to one salt bridge with Arg64 (chain A). Also, several hydrophobic interactions with the active site residues were observed in (Fig. 4).

Liver enzymes

The data analysis of the effect of methotrexate and garden cress oil on rat liver enzymes and the change percent between the MTX group and GCO two doses are shown in Fig. 5. Methotrexate significantly increased ($P \leq 0.05$) serum ALT, AST, and ALP levels compared to the control group. In contrast, the administration of garden cress oil showed a significant dose-dependent decrease in ALT, AST, and ALP levels ($P \leq 0.05$) compared to methotrexate.

Peak	Rt (min.)	RI _{exp.}	RI _{theoretical}	Identification	Molecular weight	Molecular formula	Area %
Terpenes							
1.	6.8	955	940	α-Pinene	136	C ₁₀ H ₁₆	0.016
2.	8.02	1040	1030	β-Phellandrene	136	C ₁₀ H ₁₆	0.004
3.	9.15	1052	1038	Ocimene	136	C ₁₀ H ₁₆	0.003
4.	9.6	1061	1042	Cymene	134	C ₁₀ H ₁₄	0.009
5.	9.75	1063	1044	Limonene	136	C ₁₀ H ₁₆	0.087
6.	9.82	1075	1059	Cineol	154	C ₁₀ H ₁₈ O	0.011
7.	21.45	1428	1433	Caryophyllene	204	C ₁₅ H ₂₄	0.033
8.	21.8	1431	1442	Farnesene	204	C ₁₅ H ₂₄	0.011
9.	23.08	1480	1500	Cuparene	202	C ₁₅ H ₂₂	0.027
10.	23.2	1490	1505	Cuprenene	204	C ₁₅ H ₂₄	0.011
11.	23.75	1500	1510	Bisabolene	204	C ₁₅ H ₂₄	0.734
12.	24.14	1520	1522	Sesquiphellandrene	204	C ₁₅ H ₂₄	0.027
13.	25.69	1579	1573	Caryophyllene oxide	220	C ₁₅ H ₂₄ O	0.066
14.	26	1607	1593	Carotol	222	C ₁₅ H ₂₆ O	1.1
15.	27.07	1651	1656	Daucol	238	C ₁₅ H ₂₆ O ₂	0.05
16.	36.92	2122	2118	Phytol	296	C ₂₀ H ₄₀ O	1.30
17.	48.63	2840	2790	Squalene	410	C ₃₀ H ₅₀	1.04
18.	56.5	3401	3337	β-amyrin	426	C ₃₀ H ₅₀ O	0.04
19.	57.12	3440	3425	Cycloartenol	426	C ₃₀ H ₅₀ O	0.02
Total terpenes							4.75
Phenylpropanoids							
20.	20.3	1330	1319	Methyl cinnamaldehyde	146	C ₁₀ H ₁₀ O	0.06
21.	27.98	1691	1676	Asarone < (E)->	208	C ₁₂ H ₁₆ O ₃	0.44
Total phenylpropanoids							0.5
Alkane hydrocarbons							
22.	18.03	1110	1106	Dodecane	170	C ₁₂ H ₂₆	0.002
23.	19.5	1255	1250	Methyl dodecane	184	C ₁₃ H ₂₈	0.003
24.	20.8	1427	1413	n-Tetradecane	198	C ₁₄ H ₃₀	0.02
25.	28.40	1709	1700	n-Heptadecane	240	C ₁₇ H ₃₆	0.27
26.	29.6	1764	1746	2-Methylheptadecane	254	C ₁₈ H ₃₈	0.2
27.	30.5	1801	1810	n-Octadecane	254	C ₁₈ H ₃₈	0.36
28.	31.7	1861	1845	2-Methyloctadecane	268	C ₁₉ H ₄₀	0.3
29.	32.63	1904	1910	n-Nonadecane	268	C ₁₉ H ₄₀	0.75
30.	33.47	1945	1945	9-Methylnonadecane	282	C ₂₀ H ₄₂	0.93
31.	34.85	2012	2009	n-Eicosane	282	C ₂₀ H ₄₂	1.6
32.	35.8	2044	2045	10-Methyllicosane	296	C ₂₁ H ₄₄	1.07
33.	36.12	2079	2077	n-Octadecanol	270	C ₁₈ H ₃₈ O	1.4
34.	36.62	2106	2109	n-Heneicosane	296	C ₂₁ H ₄₄	1.1
35.	37.64	2162	2173	3-Methylheneicosane	310	C ₂₂ H ₄₆	3.4
36.	38.4	2204	2208	n-Docosane	310	C ₂₂ H ₄₆	2.5
37.	38.8	2225	2210	Octadecanol acetate	312	C ₂₀ H ₄₀ O ₂	0.82
38.	39.1	2243	2246	6-methylDocosane	324	C ₂₃ H ₄₈	2.87
39.	39.88	2285	2260	Eicosenol	296	C ₂₀ H ₄₀ O	15.01
40.	40.99	2349	2300	n-Tricosane	324	C ₂₃ H ₄₈	2.62
41.	41.55	2379	2365	2-Methyltricosane	338	C ₂₄ H ₅₀	2.37
42.	41.76	2393	2375	n-Heptadecylcyclohexane	322	C ₂₃ H ₄₆	1.4
43.	42.11	2415	2400	n-Tetracosane	338	C ₂₄ H ₅₀	3.68
44.	43.36	2492	2460	13-Docosenol	324	C ₂₂ H ₄₄ O	15.13
45.	44.18	2543	2500	n-Pentacosane	352	C ₂₅ H ₅₂	2.14
46.	44.53	2565	2542	2-Methylpentacosane	366	C ₂₆ H ₅₄	4.02
47.	45.29	2614	2600	n-Hexacosane	366	C ₂₆ H ₅₄	1.99
48.	46.09	2667	2641	2-Methylhexacosane	380	C ₂₇ H ₅₆	1.32
49.	46.40	2688	2650	Tetracosanal	352	C ₂₄ H ₄₈ O	3.51
50.	46.69	2741	2700	n-Heptacosane	380	C ₂₇ H ₅₆	1.86
51.	47.3	2768	2740	2-Methylheptacosane	394	C ₂₈ H ₅₈	3.8

Continued

Peak	Rt (min.)	RI _{exp.}	RI _{theoretical}	Identification	Molecular weight	Molecular formula	Area %
52.	48.20	2809	2800	n-Octacosane	394	C ₂₈ H ₅₈	1.32
53.	49.01	2868	2840	3-Methyloctacosane	408	C ₂₉ H ₆₀	1.05
54.	49.45	2906	2900	n-Nonacosane	408	C ₂₉ H ₆₀	0.71
55.	50.5	3004	3000	n-Triacontane	422	C ₃₀ H ₆₂	0.36
56.	52	3080	3060	Hexamethyl-tetracosahexaen-3-ol	426	C ₃₀ H ₅₀ O	0.29
57.	52.25	3105	3100	n-Untriacontane	436	C ₃₁ H ₆₄	0.09
Total alkane hydrocarbons							80.26
Tocopherols							
58.	51.6	3030	3040	β/γ-Tocopherol	416	C ₂₈ H ₄₈ O ₂	0.07
59.	52.91	3155	3138	α-Tocopherol (vitamin E)	430	C ₂₉ H ₅₀ O ₂	0.009
Total tocopherols							0.079
Sterols							
60.	52.83	3130	3110	Cholesterol	386	C ₂₆ H ₄₂ O ₂	0.01
61.	53.2	3165	3144	Ergosta-5,22-dien-3-ol	398	C ₂₈ H ₄₆ O	0.08
62.	54	3230	3165	Campesterol	400	C ₂₈ H ₄₈ O	0.188
63.	54.86	3292	3230	Stigmasterol	412	C ₂₉ H ₄₈ O	0.10
64.	55.4	3296	3235	Sitosterol	414	C ₂₉ H ₅₀ O	1.13
65.	56.09	3360	3315	Stigmasta-5,24(28)-dien-3-ol	412	C ₂₉ H ₄₈ O	0.09
Total sterols							1.59
Lignans							
66.	53.4	3199	3150	Sesamin	354	C ₂₀ H ₁₈ O ₆	0.97
67.	54.4	3256	3208	Sesamolin	370	C ₂₀ H ₁₈ O ₇	1.5
Total lignans							2.47
Total identified compounds							89.5

Table 1. Relative area percentage of unsaponifiable components detected in garden cress seed oil (*Lepidium sativum*) via GC/MS analysis.

Peak	Rt (min.)	Identification	Area %
1.	33.1	Palmitic acid, methyl ester	6.85
2.	36.5	Linoleic acid, methyl ester	30.97
3.	36.7	Oleic acid, methyl ester	33.1
4.	37.1	Stearic acid, methyl ester	4.19
5.	37.38	Vaccenic acid, methyl ester	7
6.	43.6	Erucic acid, methyl ester	9.9
Total			92.02%
Saturated fatty acids			11.04%
Unsaturated fatty acids			80.98

Table 2. Relative area percentage of fatty acid methyl esters detected in garden cress seed oil (*Lepidium sativum*) via GC/MS analysis.

mRNA expression of inflammatory and apoptotic genes

Figures 6A–D present the Bax, Caspase-3, TNF, and TP53 gene expression in the liver of all experimental groups, and Fig. 6E denotes the comparison of changes in percentage gene expression between the methotrexate group and the garden cress oil-treated groups. Injection with MTX induced a significant increase in the mRNA expression level of TNF α , a proinflammatory marker, compared to the control groups ($P \leq 0.05$). However, treatment with GCO (200 and 400 mg/kg) led to a significant downregulation ($P \leq 0.05$) of TNF α compared to the MTX-treated group. Nevertheless, TNF α expression remained significantly higher among rats treated with GCO/MTX compared to the control group (Fig. 6A). Next, we analyzed the expression levels of the pro-apoptotic genes (Bax, P53, Caspase-3). The results showed that MTX caused a significant increase in Bax, P53, and Caspase-3 expression ($P \leq 0.05$). However, treatment with GCO (200 and 400 mg/kg) effectively reversed these effects ($P \leq 0.05$) (Fig. 6B–D).

Histological results

The microscopic examination of the liver section of control rats (Fig. 7A) showed a normal structure of the hepatic lobule, with cords of hepatic cells radiating from the central vein separated by blood sinusoids. In contrast, the

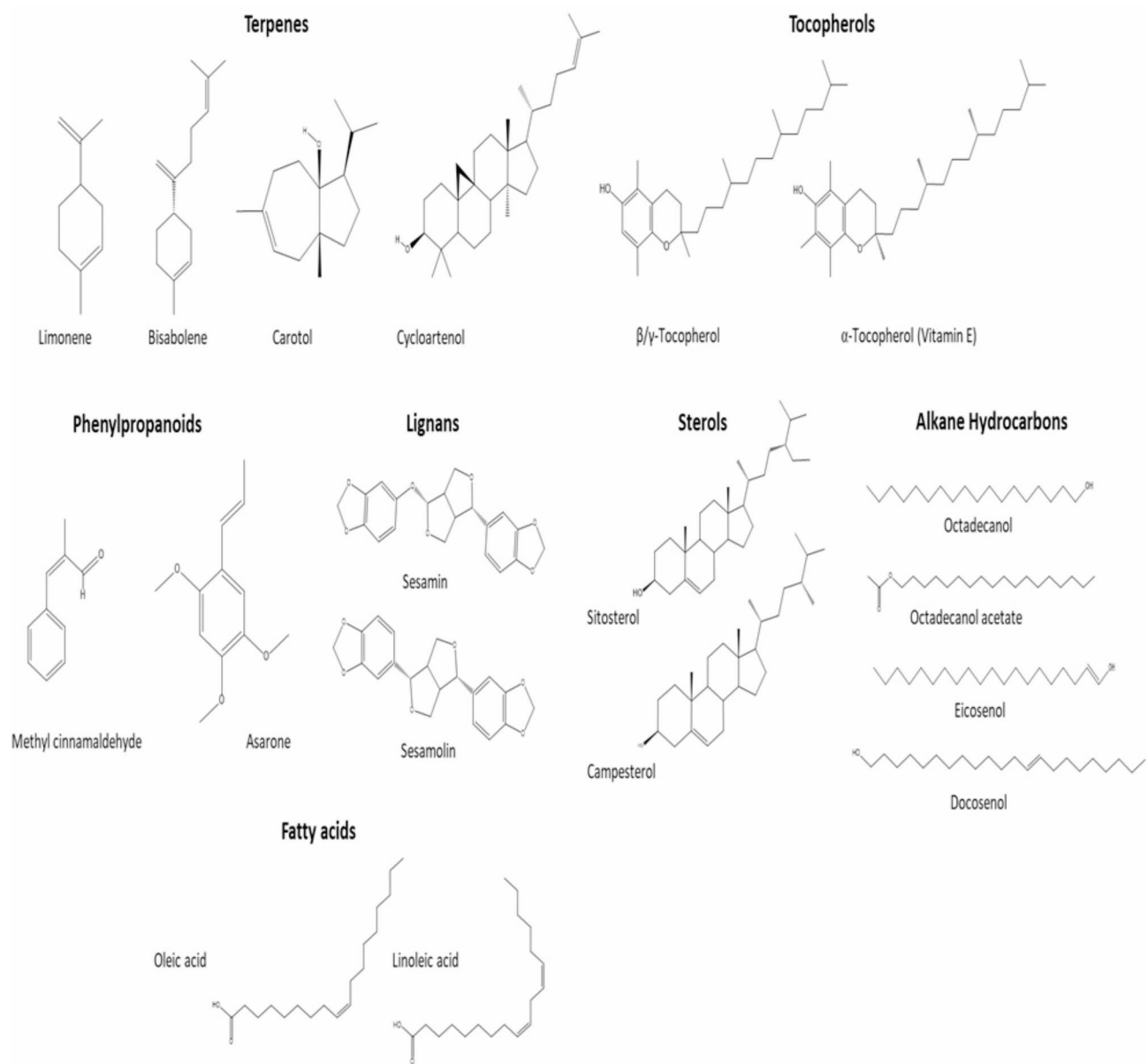


Fig. 2. Structures of selected compounds identified in garden cress seed oil via GC/MS analysis of unsaponifiable matter and fatty acids (as methyl esters).

TNF- α (PDB: 7JRA)		Caspase-3 (PDB: 3GJQ)	
Ligand	Binding energy ΔG (kcal/mol)	Compound	Binding energy ΔG (kcal/mol)
Co-crystallized inhibitor	-12.89	Co-crystallized inhibitor	-11.01
β -Tocopherol	-10.73	Linoleic acid	-10.05
Erucic acid	-9.97	Vaccenic acid	-7.48
Sesamolin	-9.91	Oleic acid	-7.45
α -Tocopherol	-9.55	Stearic acid	-6.93
γ -Tocopherol	-9.52	Palmitic acid	-6.89

Table 3. Docking results scoring Garden cress oil identified phytoconstituents against TNF- α and Caspase-3 binding sites.

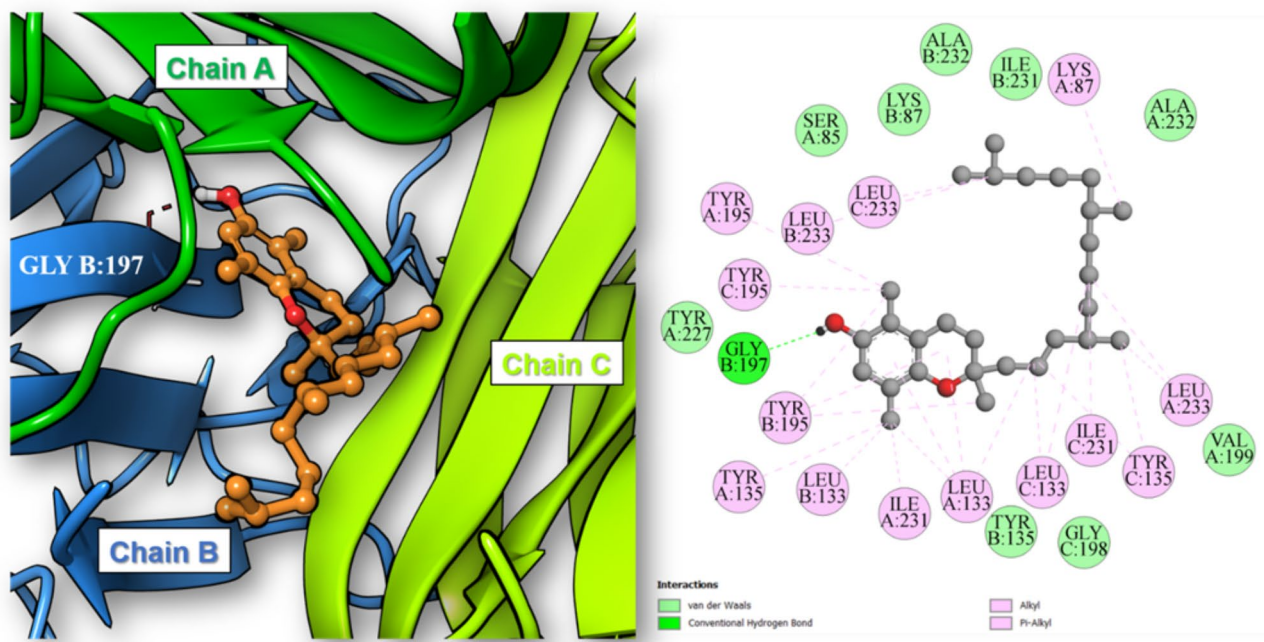


Fig. 3. 3D and 2D illustration of the docking pose and binding interactions of β -tocopherol (ball and sticks) in the active site of TNF- α homotrimer (pdb: 7JRA).

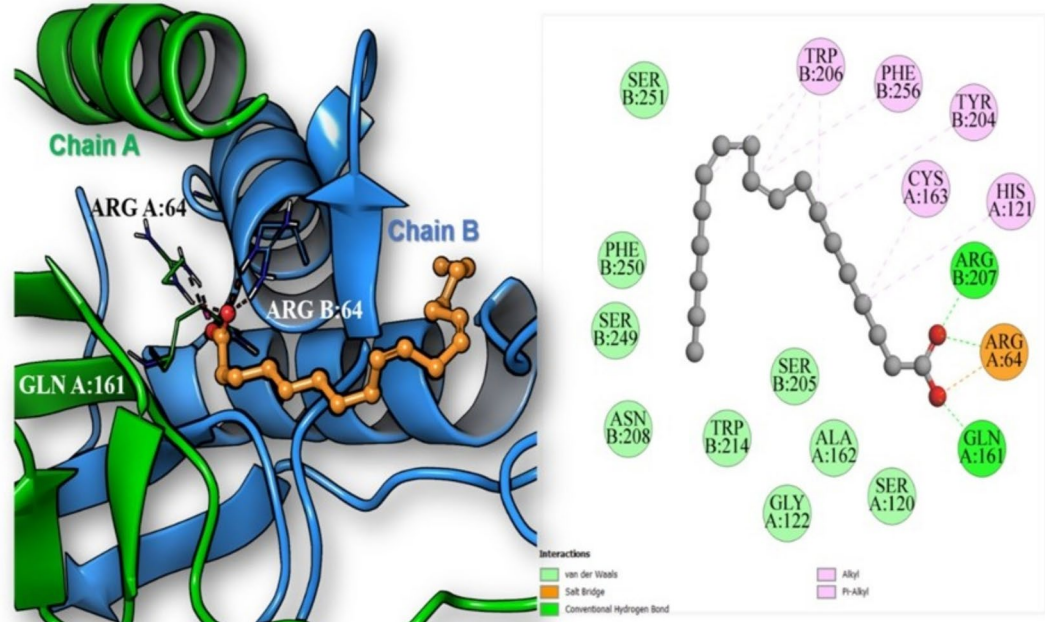


Fig. 4. 3D and 2D illustration of the docking pose and binding interactions of linoleic acid (ball and sticks) in the active site of caspase-3 heterodimer (pdb: 3GJQ).

treated rats with Garden cress seed oil extraction showed hepatic lobules that were almost normal, except for some inflammatory cells infiltrating between the sinusoids (Fig. 7B). Animals treated with methotrexate (MTX) exhibited marked cellular infiltration and septa of fibrosis around portal tracts, with shrinking hepatic cells containing pyknotic small nuclei and eosinophilic cytoplasm (Fig. 7C). Various forms of nuclear damage were

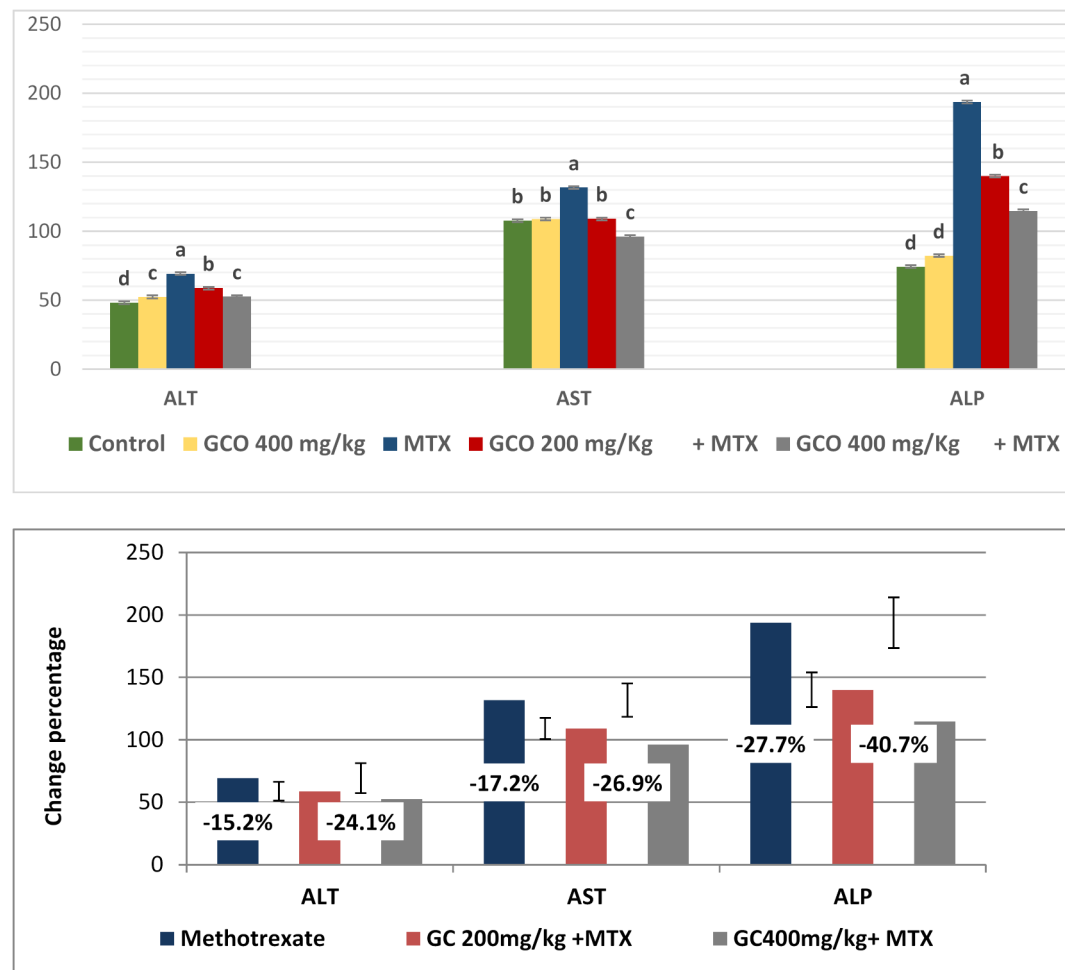


Fig. 5. Effect of methotrexate and garden cress oil on liver enzymes. Data are expressed as mean \pm SE ($n=6$). Groups with unlike superscript letters in each raw were significantly different at ($P \leq 0.05$).

present, including apoptosis and polymorphism (uneven size of the nuclei), pyknosis, karyolysis, karyorrhexis, and necrotic areas (Fig. 7D).

The livers of animals treated with MTX and garden cress seed oil at a dose of 200 mg/kg showed some improvement, such as a reduction in fibrosis around the portal area, infiltration of inflammatory cells, and dilation of sinusoids (Fig. 7E). Hepatocyte vacuolization, fatty degeneration, and focal necrotic areas (Fig. 7F) were also present. In the group treated with MTX plus garden cress oil at a dose of 400 mg/kg, there was much improvement, with a reduction in connective tissue around the portal tract, proliferation of bile ducts, and cellular infiltration (Fig. 7G). However, nuclear degeneration in the form of pyknosis, karyolysis, as well as marked vacuolar degeneration and fatty degeneration of hepatocytes, were still observed (Fig. 7H).

Van Gieson's stain is a simple method used for differential staining of collagen in connective tissue. It gives collagen a pink color, similar to what is seen in fibrosis. In control animals, the liver showed a normal distribution of fibrous tissue around the portal area (Fig. 8A). However, livers treated with Garden cress exhibited a slight increase in fibrosis around the portal tract (Fig. 8B). The group treated with MTX showed a significant increase in fibrous tissues around the portal tract, along with bile duct proliferation, massive cellular infiltration, and severe dilation of the portal area (Fig. 8C). Animals treated with MTX in combination with garden cress extract at a dose of 200 mg/kg showed some improvement, with a decrease in fibrous tissue, although dilation was still present (Fig. 8D). The group treated with MTX and garden cress seed oil at a dose of 400 mg/kg showed even more improvement, with a reduction in connective tissue around the portal tract (Fig. 8E).

Discussion

Methotrexate is the cornerstone of treatment for autoimmune diseases and a crucial part of managing inflammatory rheumatic disorders. Prescribers considering starting long-term methotrexate therapy for their patients have long been concerned about hepatotoxicity^{27,28}. *Lepidium sativum*, or garden cress is an overlooked edible herb native to Egypt and commonly cultivated worldwide. The seed oil is reported to have beneficial health-promoting effects in metabolic disorders like diabetes and hyperlipidemia, as well as antioxidant, anti-inflammatory, and antirheumatic activities²⁹. Other studies have reported in vitro and in vivo hepatoprotective

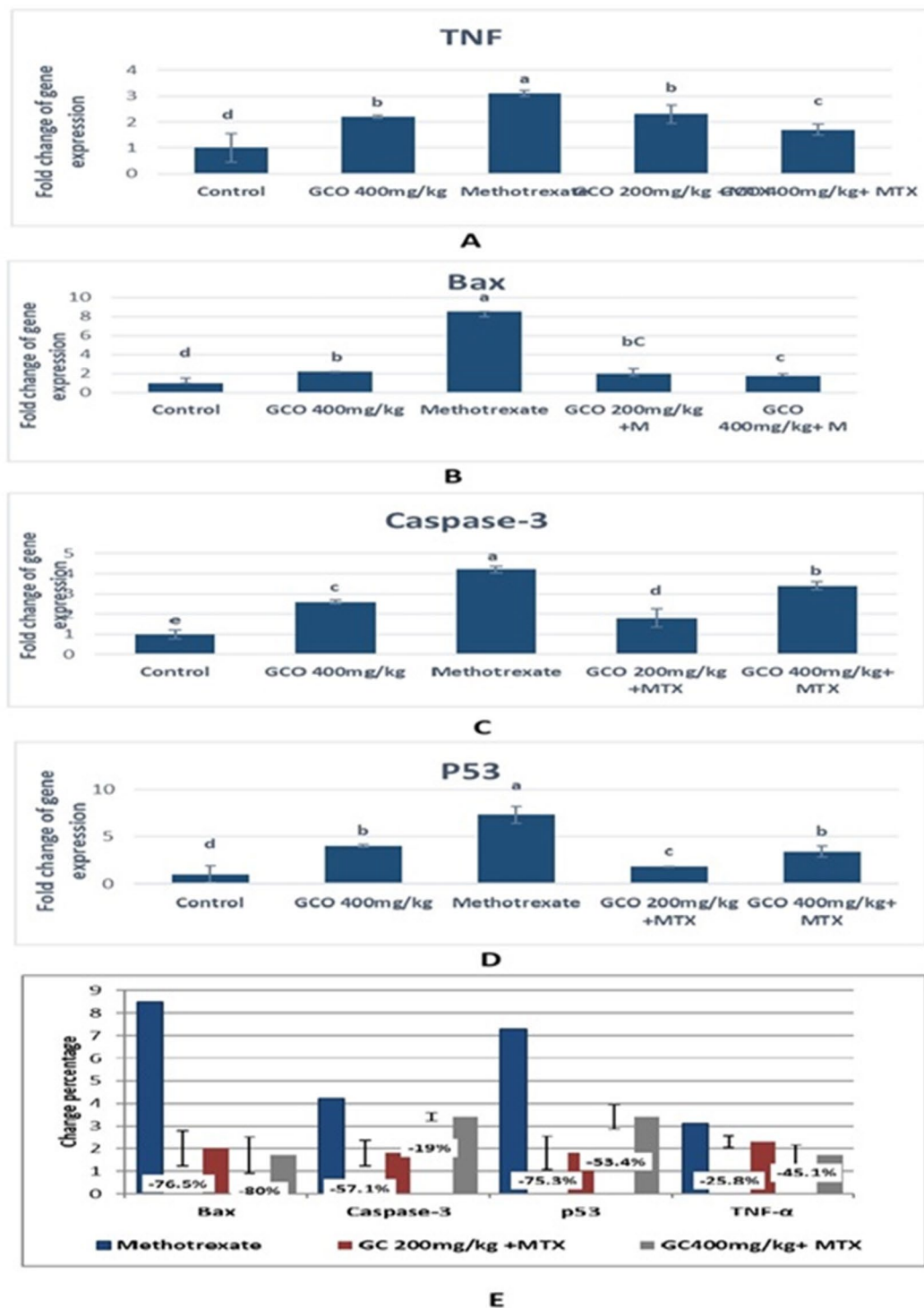
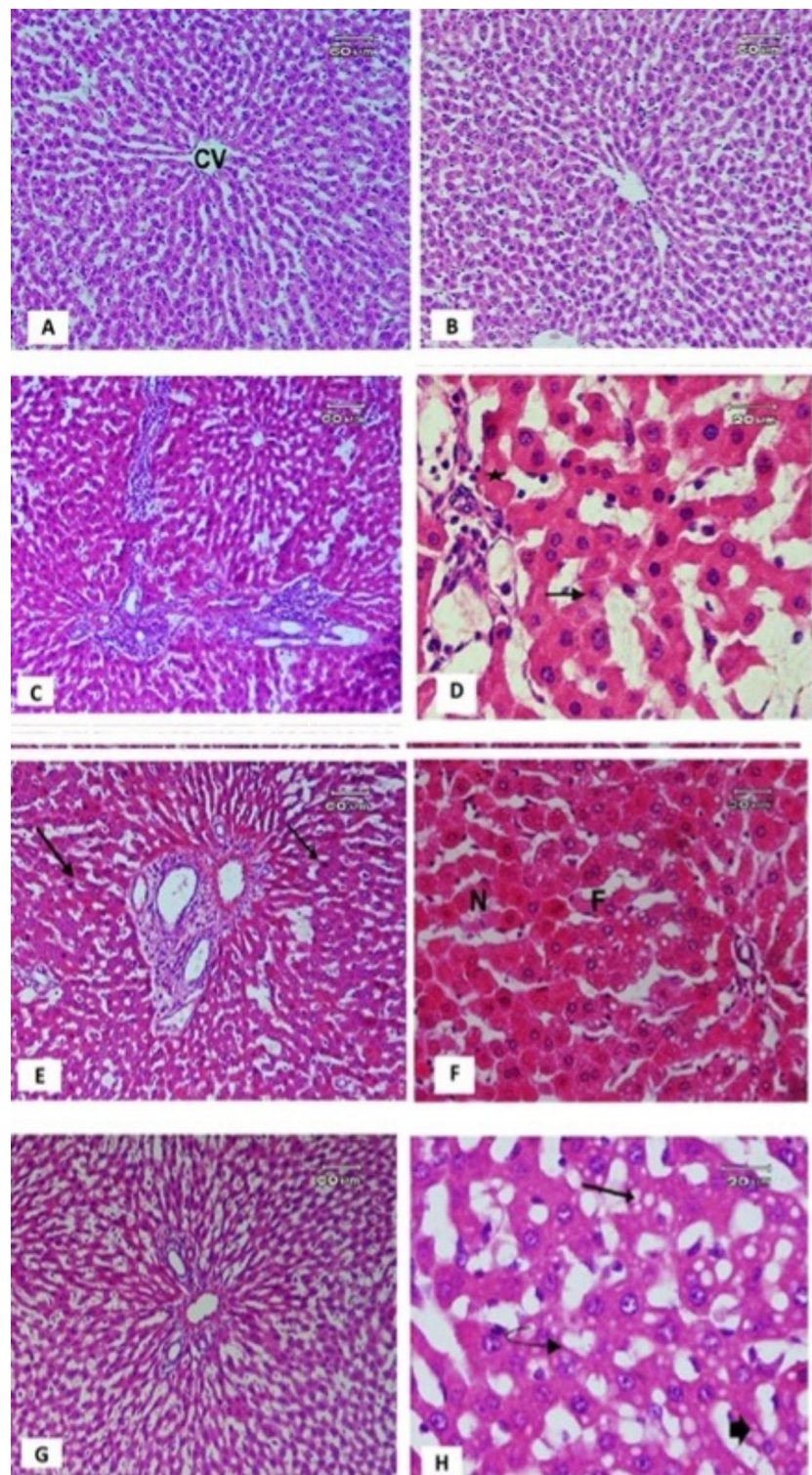


Fig. 6. The relative fold changes of inflammatory and apoptotic genes expression and the percentage change between the methotrexate and the garden cress oil-treated groups. Data are expressed as mean \pm SE ($n = 3$) for all tested groups. Groups with different superscript letters were significantly different ($P \leq 0.05$).

effects, prevention of hepatocarcinogenesis, anticarcinogenic activity, and detoxification of carcinogens by the seed extracts/juice^{30,31}. Garden cress (*Lepidium sativum*) seeds' nutritional, ethnopharmacological, and medicinal relevance might be owed to their content of bioactive compounds and antioxidant properties³².

The phytochemical investigation of commercial GCO via GC/MS analysis revealed the presence of 67 unsaponifiable compounds [19 mono-/sesqui-/di-/and tri-terpenes (4.75%), 2 phenyl propanoids (0.5%), 3 tocopherols (0.08%), 2 lignans (2.47%), 6 sterols (1.59%), 35 alkane hydrocarbons (80.26%)]. These findings are consistent with previously reported literature^{33–35}. The oil itself is odorless, but, its unsaponifiable fraction has



a characteristic aromatic scent attributed to the detected mono- and sesqui-terpenes. Additionally, 6 fatty acids were identified, with oleic and linoleic acids being the major ones. Several metabolites (Carotane sesquiterpenes, carotol, daucol, bisabolene, cuparene and cupranene) were reported for the first time in this study.

According to the liver function analysis, MTX induced liver damage, as evidenced by elevated ALT, AST, and ALP enzyme activities. These findings were consistent with those of Abdul Kadhim et al.³⁶, who linked the structural damage of the liver to increased levels of livers enzymes. Such enzymes are located in the cytoplasm and are released into the bloodstream following cellular damage, which signifies the onset of hepatotoxicity. In the investigation, we are studying the role of garden cress in attenuating the hepatotoxicity of MTX through inflammatory and apoptotic gene pathways as well as histopathological observations. Most drugs are metabolized by the liver and kidneys, making the liver susceptible to drug-induced liver injury (DILI)³⁷. In hepatocytes, methotrexate (MTX) is converted to MTX-polyglutamate (MTX-PGs) by folylpolyglutamate

◀ **Fig. 7.** Section of rat liver (A) control showing normal structure of hepatic lobule, hepatic cells radiated from central vein (CV) and sinusoids in between, (B) treated with garden cress showing hepatic lobule almost normal, while some inflammatory cells infiltration in between sinusoids were noticed. (C) Methotrexate showing marked cellular infiltration and septa of fibrosis around portal tracts, shranked hepatic cells with pyknotic small nuclei and eosinophilic cytoplasm. (D) High power of liver section treated with methotrexate showing apoptotic cells (arrow) and different form of nuclear damage represented in polymorphism (uneven size of the nuclei), pyknosis, karyolitic, karyorrhexis as well as necrotic areas (star). (E) Methotrexate plus (200 mg/Kg) Garden cress extract showing some improvement represented in reduction in fibrosis around portal area, while the thickening of the portal tract with infiltration of inflammatory cells as well as dilation of sinusoid is present. (F) High power of liver section treated with methotrexate along with Garden cress at dose (200 mg/kg) showing hepatocyte vacuolization, fatty degeneration (F) and focal necrotic areas (N). (G): methotrexate plus Garden cress extract at dose (400 mg/Kg) showing much improvement manifested by reduction of connective tissue around portal tract, proliferation of bile ducts and cellular infiltration. Meanwhile the damage of hepatic cells and necrotic areas still present. (H): High power of section of liver treated with methotrexate plus Garden cress extract at dose (400 mg/Kg) showing of nuclear degeneration in the form of (pyknosis, karyolitic (curved arrow), as well as, marked vacuolar degeneration (arrow) and fatty degeneration (thick arrow) of hepatocytes still found (Hx and E).

synthase (PGS) leading to apoptosis, fibrosis, oxidative stress, inflammation, and steatosis. The up-regulation of TNF- α observed in our study is a relevant biomarker associated with the inflammation pathway in MTX-induced hepatotoxicity. This significant increase in hepatic TNF- α may be due to MTX-PG-induced intracellular ROS, which in turn activate transcription factors like NF- κ B and Nrf-2. Their nuclear translocation causes pro-inflammatory responses through the release of several inflammatory cytokines, such as TNF- α ². Consistent with our findings, previous studies have reported that the anti-inflammatory property of *L. sativum* was attributed to the lowering of TNF- α levels³⁸. Ahmed et al.³⁹ showed that *Lepidium sativum* polysaccharides (LSP) have the potential to modulate inflammatory mediator TNF- α in septic mice. Another study by Abdulkalek et al.⁴⁰ showed that *L. sativum* seed extract could alleviate inflammatory and insulin sensitivity deviations in the liver of high-fat diet rats. Notably, our research findings demonstrated that GCO inhibited MTX-induced hepatic inflammation by lowering TNF- α mRNA expression. The anti-inflammatory effect of GCO is likely attributed to the antioxidant and/or anti-inflammatory activities of the reported bioactive components such as phenyl propanoids, α -Linolenic acid, sterols, and triterpenes²⁶. Forms of vitamin E such as γ -tocotrienol, γ -tocopherol, and δ -tocopherol are potent natural therapeutic antioxidants with anti-inflammatory properties that help prevent many illnesses⁴¹. Both lignans (sesamin and sesamolin) are reported to have antioxidant, immunomodulatory and anti-inflammatory activities as well as beneficial health promoting effect on decreasing hepatic lipogenic activity through increasing fatty acid oxidation enzymes⁴². Furthermore, a recent study found that oleic and palmitic acids have anti-inflammatory and antimicrobial activities. They achieve this by reducing the expression of TNF in lipopolysaccharide-stimulated macrophages⁴³.

Regarding apoptotic markers, MTX resulted in significantly higher expression levels of Bax, caspase-3, and P53 genes. Our results support previous studies that have shown increased expression levels of these genes in vivo in response to MTX^{44–46}. During MTX-induced hepatotoxicity, an increase in oxidative stress leads to Bax translocation to the outer mitochondrial membrane, resulting in increased mitochondrial permeability and cytochrome c release into the cytosol. This activates downstream effector caspases, such as caspase-3⁴⁷. Conversely, our results indicated that GCO downregulated the elevation of Bax, Caspase-3, and P53 induced by MTX in rat liver tissue, explaining its antiapoptotic action. These findings are consistent with Raish et al.⁴⁸, who reported that *Lepidium sativum* ethanolic extract significantly down-regulated the expression levels of caspase-3 in a galactosamine/lipopolysaccharide-induced liver damage model. Additionally, oleic acid, a constituent of GCO, showed a decrease in the expression of caspase-3, Bcl-2, and Bax, thereby inhibiting hepatocyte apoptosis⁴⁸.

The in silico docking study of the identified metabolites into TNF- α (pdb: 7JRA) and Caspase-3 (pdb: 3GJQ) target proteins suggested that the observed anti-inflammatory activity of GCO through inhibition of TNF- α enzyme could be attributed to tocopherols (α -/ β -/ and γ), sesamolin lignan, and erucic acid. These compounds showed the highest binding affinity, with docking scores ranging from 9.52 to 10.73 kcal/mol, compared to the co-crystallized ligand (12.89 kcal/mol). Tocopherols, especially vitamin E, and sesamolin were reported to attenuate TNF- α gene expression and improve the treatment of hepatotoxicity⁴⁹. Linoleic acid showed the highest docking score against caspase-3 protein (10.05 kcal/mol) compared to its co-crystallized ligand (11.01 kcal/mol), followed by other fatty acids. Kabakci and Bozkir et al.⁴⁵ demonstrated that linoleic acid has a protective effect on methotrexate-induced liver toxicity by modulating the expression of apoptotic pathway mediators such as Bax, Bcl-2 and Caspase-3. Linoleic acid was found to attenuate acute liver injury associated with lipopolysaccharide by alleviating histopathological abnormalities and liver enzymes, as well as inhibiting proinflammatory markers such as TNF- α and IL-6⁵⁰.

The histological analyses revealed significant liver damage in the MTX-treated group, including interface necrosis, apoptotic cells, and central zone lymphocyte infiltration. These alterations are corroborated by previous research⁵¹. Morsy et al.¹³ demonstrated that rats receiving MTX showed high collagen deposition in their liver tissue, primarily leading to hepatic fibrosis. Taskin et al.⁵² confirmed that MTX exhibited many pathological anomalies in the liver, including hepatocyte necrosis, fibrosis, and an increase in cellular infiltration. In response to apoptosis, cells undergoing necrosis lose membrane integrity and release their intracellular components, serving as danger signals that trigger inflammation⁵³. Van Loo and Bertrand⁵⁴ discovered that TNF induces inflammatory responses by directly stimulating the expression of inflammatory genes and indirectly by

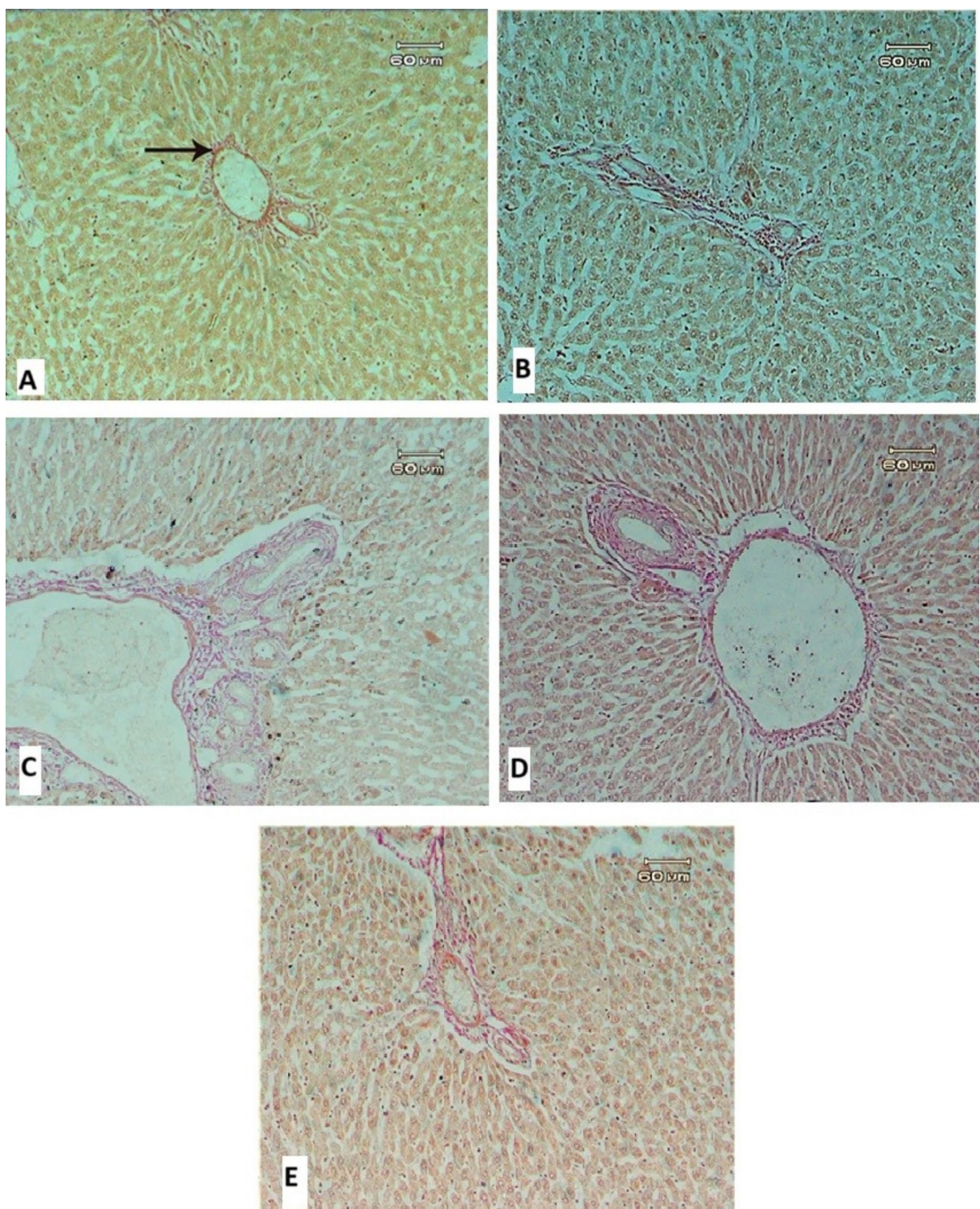


Fig. 8. Image (A): Liver section of control rat showing normal distribution of fibrous tissue around portal area (arrow). (B) Liver section of rat treated with garden cress showing minimal amount of fibrous tissue and slight dilation in portal area. (C) Liver treated with methotrexate showing severe dilation of portal area and increase in fibrous tissues around portal tract, proliferation of bile ducts and massive cellular infiltration. (D) Liver treated with methotrexate pulse garden cress extraction at dose (200 mg/kg) showing some improvement represented in decrease in fibrous tissue while the dilation still present (E) Liver treated with methotrexate pulse Garden cress extraction at dose (400 mg/kg) showing much improvements represented in reduction in fibrous tissues around portal tract.

promoting inflammatory immune responses and cell death. These findings support the upregulation of TNF- α mRNA expression in groups treated with MTX.

Meanwhile, the present study indicated that garden cress restores the histopathological alterations induced by MTX. According to Zamzami et al.⁵⁵, *Lepidium sativum* enhanced liver function in CCl₄-treated New Zealand white rabbits by reversing the liver histopathologic alterations. Additionally, Ibrahim et al.⁵⁶ reported that a daily dose of 400 mg/kg b.w. of garden cress ethanolic extract has hepatoprotective, antioxidant, and anti-steatosis properties in rats. Garden cress has been found to have potential benefits for liver tissue regeneration, where bioactive compounds in the seeds are thought to promote the growth of new liver cells, aiding in the restoration of injured liver tissue⁵⁷. On the other hand, the liver of rats treated with garden cress oil showed very few inflammatory cells penetrating between the sinusoids. This finding was supported by Abuelgasim et al., who reported that the rats administered 400 mg/kg (Bwt) showed scarred vacuolated cells and hepatic congestion⁵⁸.

Conclusion

All of our data points to the fact that GCO protects the liver from MTX-induced damage. This is partially explained by its strong anti-inflammatory, anti-fibrotic, and anti-apoptotic properties. These properties are probably attributed to the active compounds present in GCO that were recognized from our in-silico study as compounds for attenuating the inflammatory and apoptosis reactions in the liver by inhibiting TNF- α and caspase-3, as proven by gene expression results.

Materials and methods

Chemicals

Methotrexate was obtained from EIMC United Pharmaceuticals Company (Cairo-Egypt). Cold-pressed Garden cress oil was purchased from Haraz Co., Cairo, Egypt. All other chemicals were of analytical grade and acquired from standard marketable suppliers.

GC/MS analysis of lipid content in garden cress seed oil

Saponification of garden cress oil (GCO) (8 g) was performed by refluxing for 6–8 h with alcoholic KOH, followed by extraction of unsaponifiable matter with ether, yielding 0.7 g upon evaporation to dryness. Fatty acids were methylated through reflux with a 2 M HCl solution in methanol for 3–4 h, then extracted with ether and evaporated to dryness, yielding 4.8 gm as fatty acid methyl esters (FAME)⁵⁹.

Both fractions were then analyzed via a Shimadzu GCMS-QP2010 (Kyoto, Japan) equipped with an Rtx-5MS fused bonded column (30 m × 0.25 mm i.d. × 0.25 μ m film thickness) (Restek, USA) with a split–splitless injector. The following guidelines were established: the initial temperature of the column was maintained at 50 °C for three minutes (isothermal), then it was increased to 300 °C at a rate of 5 °C per minute and held there for ten minutes (isothermal). Even though the injector temperature was established at 280 °C. The flow rate of the helium carrier gas was 1.37 ml/min. The following parameters were applied to all mass spectra recordings: Ion source temperature: 220 °C; ionization voltage: 70 eV; filament emission current: 60 mA. Split mode injections were used with diluted samples (1% v/v; split ratio: 1:15). Identification of compounds was achieved by comparing their retention index (RI) and mass spectral data with NIST/Wiley, Pherobase, and other literature sources⁶⁰.

Molecular docking study of identified compounds

The 3D coordinates of the detected phytoconstituents were obtained in SDF format from the PubChem database. After being energy-minimized to a gradient of 0.01 kcal/mol Å in the gas phase using the MMFF94x Force Field, the data were saved in PDBQT format. Human TNF- α (PDB ID: 7JRA) and human caspase-3 (PDB ID: 3GJQ) co-crystal structures were obtained from the Protein Data Bank (<https://www.rcsb.org>). Using MGL Tools v1.5.7, all target receptors were prepared by deleting water molecules and other heteratoms, adding polar hydrogens, and assigning Kollman charges. The receptors were then saved in PDBQT format. Grid boxes measuring 25 × 25 × 25 Å were positioned at the co-crystallized ligands to encompass the entire binding sites of the target receptors. To perform all docking computations, AutoDock Vina, an open-source program, was utilized. The docking poses were ranked according to their docking scores, and the pose with the best energy was selected. Using Discovery Studio Visualizer v21.1.0.20298, the interactions between the selected compounds and the target proteins were examined⁶¹.

In vivo experimental design

Thirty adult male Sprague–Dawley albino rats, weighing between 100 to 150 g, were obtained from the animal facility at the National Research Center in Giza, Egypt. The rats were housed in a room with controlled environmental conditions, including a 12-h light/12-h dark cycle and a temperature of 22 °C. They were kept in clear plastic cages with stainless steel wire tops, and provided with rat feed pellets and unrestricted access to water. The study was approved by the Ethics Committee at the National Research Center (Approval No. 09410125). The research methods were carried out following relevant guidelines and ARRIVE guidelines.

The rats were randomly divided into five groups, each consisting of six animals. The animals were given a week to acclimate before the start of the study. The groups were as follows: Group I: rats received oral gavages of saline as a negative control. Group II: animals were orally administered Garden cress oil (400 mg/kg/day) for 28 days as a vehicle group. Group III: animals were intraperitoneally injected with methotrexate at a dose of 5 mg/kg/day for 7 days following the protocol of Demiryilmaz et al.⁶². Groups IV & V: animals were injected with methotrexate following the same protocol as Group III. On the eighth day, they were orally administered garden cress oil at doses of 200 and 400 mg/kg once daily for 28 days, as described by Yogesh et al.⁶³.

Gene	Primer forward	Primer reverse	Product size	Accession No
Caspase	ATTGACACAATACACGGGATCTGT	AAATTCAAGGGACGGGTCA	183	NM_012922.2
Bax	AGA GGA TGA TTG CTG ATG TGG	CCC AGT TGA AGT TGC CGT	93	NM_017059.2
P53	GCA GAG TTG TTA GAA GGC	TTG AGA AGG GAC GGA AGA	138	NM_030989.4
TNF	CCACCAACGCTCTGTCTAC	ACCACCAAGTTGGTTGTCTTG	256	NM_012675.3
GAPDH	AACTTGGCATTGTGGAAGG	ACACATTGGGGTAGGAACA	223	NM_017008.4

Table 4. Primers of candidate genes.

Blood and tissue sampling

At the end of the experiment, rats were anesthetized with an intraperitoneal injection of xylazine (5 mg/kg b.w.) and ketamine (50 mg/kg b.w.) (Sigma Aldrich, USA; Cat. No. K113). Following this, blood samples were taken from the heart cavity in heparinized glass tubes and centrifuged for ten minutes at 5000 rpm. Aliquots of the plasma were kept at -80 °C until analysis, once the livers had been removed and rinsed with cold saline. After that, portions of the liver were frozen in liquid nitrogen and kept at -80 °C for the real-time quantitative PCR (RT-qPCR) study. A portion of the tissue samples was kept in 10% formalin buffer for histopathological analysis.

Liver enzymes assessment

Serum alanine aminotransferase (ALT), aspartate aminotransferase (AST), and alkaline phosphatase (ALP) activities were measured in all blood samples. These enzymes were tested using colorimetric commercial kits from Bio Diagnostic (Egypt) according to the manufacturer's instructions.

RNA isolation, cDNA synthesis, and reverse transcription polymerase chain reaction (RT-PCR) analysis

Isolated liver samples were homogenized in an Easy Red Total RNA Extraction Kit (Intronbio, Korea), and RNA was extracted following the manufacturer's instructions. The yield and quality of isolated RNAs were assessed through gel electrophoresis and spectrophotometric measurement. The RNA was then treated with the RNase-free DNase kit (Thermo Scientific) and cDNA was synthesized via reverse-transcription as per the manufacturer's instructions (Thermo Scientific, China). Glyceraldehyde-3-phosphate dehydrogenase (GADPH) was used as the internal control and the expression of four genes (Bcl-associated X protein (Bax), cysteine aspartic acid specific protease 3 (Caspase-3), tumor necrosis factor alpha (TNF- α) and tumor-suppressor protein (P53) was evaluated in the study. RT-qPCR was conducted using the Stratagene Mx3000P Real-Time PCR System (Agilent Technologies, USA) and carried out in a 25 μ L reaction containing cDNA, TOPreal™qPCR 2X PreMIX (SYBR Green with low ROX) (Enzyomics), forward and reverse primers (10 pmol/ μ L) (Macrogen), and free water nuclease. The gene expression levels were calculated using the 2- $\Delta\Delta Ct$ method⁶⁴. The primers used for RT-qPCR above are listed in Table 4.

Histological methodology

Hematoxylin and eosin stain

The liver specimens were collected, fixed in a 10% buffered formalin (Thermo Fisher Scientific, Waltham, MA) at room temperature for one to three days, and embedded in paraffin. Subsequently, 5 μ m thick paraffin tissue sections were subjected to standard procedures, including deparaffinizing, hematoxylin and eosin staining, dehydration, and mounting were prepared and stained with H&E stain following the method of Drury and Wallington⁶⁵. Using an optical microscope (Olympus, IX53, Tokyo, Japan), the stained slides were inspected and captured on camera.

Van Gieson stain

Van Gieson stain was used to evaluate liver fibrosis, following the protocol outlined by Chen et al.⁶⁶. Briefly, paraffin-embedded liver sections were deparaffinized and hydrated in distilled water. They were then stained with Wright's Working Hematoxylin for 10 min and washed in distilled water. The slides were further stained with Van Gieson solution for 3 min, followed by gradient dehydration in 95% alcohol, absolute alcohol, and 2 changes in xylene before mounting with DPX for investigation.

Statistical analysis

The data obtained were presented as means \pm standard error of the means (SEM) ($n=3$) and analysis was performed using the SPSS 16.0 program (SPSS Inc., Chicago, IL, USA). One way analysis of variance method was used to evaluate the statistical differences. Differences among groups were considered statistically significant at p values ≤ 0.05 .

Data availability

Data is provided within the manuscript file.

Received: 1 August 2024; Accepted: 6 February 2025

Published online: 20 February 2025

References

1. Kalantari, E., Zolbanin, N. M. & Ghasemnejad-Berjeni, M. Protective effects of empagliflozin on methotrexate induced hepatotoxicity in rats. *Biomed. Pharmacother.* **170**, 115953. <https://doi.org/10.1016/j.biopha.2023.115953> (2024).
2. Ezhilarasan, D. Hepatotoxic potentials of methotrexate: Understanding the possible toxicological molecular mechanisms. *Toxicology* **458**, 152840. <https://doi.org/10.1016/j.tox.2021.152840> (2021).
3. Valerio, V. et al. Systematic review of recommendations on the use of methotrexate in rheumatoid arthritis. *Clin. Rheumatol.* **40**, 1259–1271. <https://doi.org/10.1007/s10067-020-05363-2> (2021).
4. Ikponmwosa, O. B. & Usunomena, U. Aqueous leaf extract of *Chromolaena odorata* attenuates methotrexate-induced hepatotoxicity in Wistar rats. *J. Fundam. Appl. Pharm.* **3**(1), 16–29 (2022).
5. AbdelKader, G. et al. Protective effects of crocin against methotrexate-induced hepatotoxicity in adult male albino rats: Histological, immunohistochemical, and biochemical study. *Cureus* **15**, e34468. <https://doi.org/10.7759/cureus.34468> (2023).
6. Aboubakr, M. et al. Allicin and lycopene possesses a protective effect against methotrexate induced testicular toxicity in rats. *Pak. Vet. J.* **43**, 559–566. <https://doi.org/10.29261/pakvetj/2023.057> (2023).
7. Bath, R. K., Brar, N. K., Forouhar, F. A. & Wu, G. Y. A review of methotrexate-associated hepatotoxicity. *J. Dig. Dis.* **15**, 517–524. <https://doi.org/10.1111/1751-2980.12184> (2014).
8. Tag, H. M. Hepatoprotective effect of mulberry (*Morus nigra*) leaves extract against methotrexate induced hepatotoxicity in male albino rat. *BMC Complement. Altern. Med.* **15**, 252. <https://doi.org/10.1186/s12906-015-0744-y> (2015).
9. Cao, Y. et al. Protective effects of magnesium glycyrhizinate on methotrexate-induced hepatotoxicity and intestinal toxicity may be by reducing COX-2. *Front. Pharmacol.* **1**, 119. <https://doi.org/10.3389/fphar.2019.00119> (2019).
10. Abdelaziz, R. M., Abdelazem, A. Z., Hashem, K. S. & Attia, Y. A. Protective effects of hesperidin against MTX-induced hepatotoxicity in male albino rats. *Naunyn Schmiedebergs Arch. Pharmacol.* **393**(8), 1405–1417. <https://doi.org/10.1007/s00210-020-01843-z> (2020).
11. Abd El-Ghafar, O. A. M. et al. Hepatoprotective effect of acetovanilloone against methotrexate hepatotoxicity: Role of Keap-1/Nrf2/ARE, IL6/STAT-3, and NF- κ B/AP-1 signaling pathways. *Phytother. Res. PTR* **36**(1), 488–505. <https://doi.org/10.1002/ptr.7355> (2022).
12. Alfwuaires, M. A. Galangin mitigates oxidative stress, inflammation, and apoptosis in a rat model of methotrexate hepatotoxicity. *Environ. Sci. Pollut. Res.* **29**, 20279–20288. <https://doi.org/10.1007/s11356-021-16804-z> (2022).
13. Morsy, M. A., Abdel-Latif, R., Hafez, S. M. N. A., Kandeel, M. & Abdel-Gaber, S. A. Paeonol protects against methotrexate hepatotoxicity by repressing oxidative stress, inflammation, and apoptosis-the role of drug efflux transporters. *Pharmaceutics* **15**(10), 1296. <https://doi.org/10.3390/ph15101296> (2022).
14. Wang, S. C. et al. Melatonin protects against methotrexate hepatotoxicity in young rats: Impact of PI3K/Akt/mTOR signaling. *J. Biochem. Mol. Toxicol.* **37**(5), e23323. <https://doi.org/10.1002/jbt.23323> (2023).
15. Clary, D. D., Reid, A. T., Kiani, R. & Fanciullo, J. Methotrexate hepatotoxicity monitoring guidelines in psoriasis and rheumatoid arthritis: Is there a consensus?. *South Dakota Med.* **74**(8), 363–366 (2021).
16. Azzam, A., Jiyad, Z. & O’Beirne, J. Is methotrexate hepatotoxicity associated with cumulative dose? A systematic review and meta-analysis. *Austral. J. Dermatol.* **62**(2), 130–140. <https://doi.org/10.1111/ajd.13546> (2021).
17. Feroz, W. & Sheikh, A. M. A. Exploring the multiple roles of guardian of the genome: P53. *Egypt J. Med. Hum. Genet.* **21**, 49. <https://doi.org/10.1186/s43042-020-00089-x> (2020).
18. Vahid, N. K., Nameni, F. & Chaharmahali, B. Y. Effect of interval training and curcumin on BAX, Bcl-2, and caspase-3 enzyme activity in rats. *Gene Cell Tissue* **9**(4), e112792 (2022).
19. Faletti, L. et al. TNF α sensitizes hepatocytes to FasL-induced apoptosis by NF κ B-mediated Fas upregulation. *Cell Death Dis.* **9**, 909 (2018).
20. El-Makawy, A. I. et al. Efficiency of turnip bioactive lipids in treating osteoporosis through activation of Osterix and suppression of Cathepsin K and TNF- α signaling in rats. *Environ. Sci. Pollut. Res. Int.* **27**(17), 20950–20961. <https://doi.org/10.1007/s11356-020-08540-7> (2020).
21. El-Makawy, A. I., Mabrouk, D. M., Ibrahim, F. M., Abdel-Aziem, S. H. & Sharaf, H. A. Therapeutic and prophylactic efficacy of garden cress seed oil against osteoporosis in rats. *Jordan J. Biol. Sci.* **13**(2), 237–245 (2020).
22. Kanabur, V. & Sharavathi, V. Nutritional significance and usage of garden cress seeds (*Lepidium sativum* L)-a review. *Am. J. Food Sci. Technol.* **1**(1), 50–55 (2022).
23. Lahiri, B. & Rani, R. Garden cress Seeds: Chemistry, medicinal properties, application in dairy and food industry: A Review. *Emerg. Life Sci. Res.* **6**, 1–4 (2020).
24. Emhofer, L., Himmelsbach, M., Buchberger, W. & Klampfl, C. W. High-performance liquid chromatography drift-tube ion-mobility quadrupole time-of-flight/mass spectrometry for the identity confirmation and characterization of metabolites from three statins (lipid-lowering drugs) in the model plant cress (*Lepidium sativum*) after uptake from water. *J. Chromatogr. A* **1592**, 122–132 (2019).
25. Jagdale, Y. D. et al. Nutritional profile and potential health benefits of super foods: A review. *Sustainability* **13**(16), 9240 (2021).
26. Vazifeh, S., Kananpour, P., Khalilpour, M., Eisalou, S. V. & Hamblin, M. R. Anti-inflammatory and immunomodulatory properties of *Lepidium sativum*. *Biomed. Res. Int.* **12**. <https://doi.org/10.1155/2022/3645038> (2022).
27. Abdulaziz, N. T., Mohammed, E. T., Khalil, R. R. & Mustafa, Y. F. Unrevealing the total phenols, total flavonoids, antioxidant, anti-inflammatory, and cytotoxic effects of Garden Cress seed ethanolic extracts. *Rev. Clin. Pharmacol. Pharmacokinet. Int. Ed.* **38**(2), 187–196. <https://doi.org/10.61873/AGND54328> (2024).
28. Sayed, A. A., Ali, A. M. & Bekhet, G. M. The protective effect of garden cress *Lepidium sativum* against lipopolysaccharide (LPS) induced hepatotoxicity in mice model. *Indian J. Anim. Res.* **55**(9), 1065–1071. <https://doi.org/10.18805/IJAR.B-1323> (2021).
29. Di Martino, V. et al. Busting the myth of methotrexate chronic hepatotoxicity. *Nat. Rev. Rheumatol.* **19**(2), 96–110. <https://doi.org/10.1038/s41584-022-00883-4> (2023).
30. Pradhan, A., Sengupta, S., Sengupta, R. & Chatterjee, M. Attenuation of methotrexate induced hepatotoxicity by epigallocatechin 3-gallate. *Drug Chem. Toxicol.* **46**(4), 717–725. <https://doi.org/10.1080/01480545.2022.2085738> (2023).
31. Rezig, L. et al. Profile characterization and biological activities of cold pressed Garden cress (*Lepidium sativum*) seed oil. *Arab. J. Chem.* **15**(8), 103958 (2022).
32. Nazir, S. et al. *Lepidium sativum* secondary metabolites (essential oils): In vitro and in silico studies on human hepatocellular carcinoma cell lines. *Plants* **10**(9), 2021. <https://doi.org/10.3390/plants10091863> (1863).
33. Bhatia, K. & Bhasin, A. Exploring the versatile potential of garden cress seeds: Therapeutic applications and industrial utilization: A comprehensive review. *Pharma Innov.* **12**(9), 101–108. <https://doi.org/10.22271/tpi.2023.v12.i9b.22647> (2023).
34. Ismael, I. A. & Khorsheed, A. C. Quantitative and qualitative detection of metabolic compounds in the seeds of cress plant (*Lepidium sativum* L.) using chromatography technique. *J. Kerbala Agric. Sci.* **8**(1), 8–16. <https://doi.org/10.59658/jkas.v8i1.867> (2021).
35. Abdul Kadhim, B. A., Ghafil, F. A., Qassam, H. & Hadi, N. R. Hepato-protective effects of Silymarin against methotrexate-induced hepatotoxicity in rat model. *J. Popul. Ther. Clin. Pharmacol.* **30**(1), 373–382. <https://doi.org/10.47750/jptcp.2023.1096> (2023).
36. Hosack, T., Damry, D. & Biswas, S. Drug-induced liver injury: A comprehensive review. *Ther. Adv. Gastroenterol.* **16**, 17562848231163410. <https://doi.org/10.1177/17562848231163410> (2023).
37. Turkoglu, M., Kilic, S., Pekmezci, E. & Kartal, M. Evaluating antiinflammatory and antiandrogenic effects of garden cress (*Lepidium sativum* L.) in HaCaT cells. *Rec. Nat. Prod.* **12**(6), 595–601 (2018).

38. Alqahtani, F. Y. et al. Chemical composition and antimicrobial, antioxidant, and anti-inflammatory activities of *Lepidium sativum* seed oil. *Saudi J. Biol. Sci.* **26**(5), 1089–1092. <https://doi.org/10.1016/j.sjbs.2018.05.007> (2019).
39. Ahmad, A. et al. Inhibitory effects of *Lepidium sativum* polysaccharide extracts on TNF- α production in *Escherichia coli*-stimulated mouse. *Biotech* **8**(6), 286. <https://doi.org/10.1007/s13205-018-1309-9> (2018).
40. Abdulmalek, S. A., Fessal, M. & El-Sayed, M. Effective amelioration of hepatic inflammation and insulin response in high fat diet-fed rats via regulating AKT/mTOR signaling: Role of *Lepidium sativum* seed extracts. *J. Ethnopharmacol.* **266**, 113439. <https://doi.org/10.1016/j.jep.2020.113439> (2021).
41. Ciarcià, G. et al. Vitamin E and non-communicable diseases: A review. *Biomedicines* **10**, 2473 (2022).
42. Pathak, N., Bhaduri, A. & Rai, A. K. Sesame: Bioactive compounds and health benefits. *Bioactive Mol. Food* **5**, 181–200 (2019).
43. Charlet, R., Le Danvic, C., Sendid, B., Nagnan-Le Meillour, P. & Jawhara, S. Oleic acid and palmitic acid from *Bacteroides thetaiotaomicron* and *Lactobacillus johnsonii* exhibit anti-inflammatory and antifungal properties. *Microorganisms* **2022**, 10 (1803).
44. Almalki, R. S. The protective effect of roflumilast against acute hepatotoxicity caused by methotrexate in Wistar rats: In vivo evaluation. *Drug Des. Dev. Ther.* **18**, 453–462. <https://doi.org/10.2147/DDDT.S438703> (2024).
45. Kabakci, A. G. & Bozkir, M. G. Protective effect of linoleic acid on liver toxicity induced by methotrexate. *Int. J. Morphol.* **41**(1), 237–245 (2023).
46. Kizil, H. E. et al. Morin ameliorates methotrexate-induced hepatotoxicity via targeting Nrf2/HO-1 and Bax/Bcl2/Caspase-3 signaling pathways. *Mol. Biol. Rep.* **50**, 3479–3488. <https://doi.org/10.1007/s11033-023-08286-8> (2023).
47. Mahmoud, A. M. et al. Ferulic acid prevents oxidative stress, inflammation, and liver injury via upregulation of Nrf2/HO-1 signaling in methotrexate-induced rats. *Environ. Sci. Pollut. Res.* **27**, 7910–7921. <https://doi.org/10.1007/s11356-019-07532-6> (2020).
48. Raish, M. et al. Hepatoprotective activity of *Lepidium sativum* seeds against D-galactosamine/lipopolysaccharide induced hepatotoxicity in animal model. *BMC Complement. Altern. Med.* **16**, 501. <https://doi.org/10.1186/s12906-016-1483-4> (2016).
49. Hadipour, E. & Emami, S. A. Effects of sesame (*Sesamum indicum* L.) and bioactive compounds (sesamin and sesamolin) on inflammation and atherosclerosis: A review. *Food Sci. Nutr.* **11**, 3729–3757. <https://doi.org/10.1002/fsn3.3407> (2023).
50. Zhang, Q. et al. Linoleic acid alleviates lipopolysaccharide induced acute liver injury via activation of Nrf2. *Physiol. Res.* **73**(3), 381–391. <https://doi.org/10.33549/physiolres.935201> (2024).
51. Kalantari, H., Asadmasjedi, N., Reza Abyaz, M., Mahdavinia, M. & Mohammadtaghvaei, N. Protective effect of inulin on methotrexate-induced liver toxicity in mice. *Biomed. Pharmacother.* **110**, 943–950 (2019).
52. Taskin, B., Erdogan, A. M., Yigitтурk, G., Gunenç, D. & Erbas, O. Antifibrotic effect of lactulose on a methotrexate-induced liver injury model. *Gastroenterol. Res. Pract.* **2017**, 7942531. <https://doi.org/10.1155/2017/7942531> (2017).
53. Miller, M. A. & Zachary, J. F. Mechanisms and morphology of cellular injury, adaptation, and death. *Pathol. Basis Vet. Dis.* **2017**, 2–43. <https://doi.org/10.1016/B978-0-323-35775-3.00001-1> (2017).
54. van Loo, G. & Bertrand, M. J. M. Death by TNF: A road to inflammation. *Nat. Rev. Immunol.* **23**, 289–303. <https://doi.org/10.1038/s41577-022-00792-3> (2023).
55. Zamzami, A. M., Baothman, O. A., Samy, F. & Abo-Golayel, M. K. Amelioration of CCl4-induced hepatotoxicity in rabbits by *Lepidium sativum* seeds. *Evid. Based Complement. Altern. Med.* **2019**, 17 (2019).
56. Ibrahim, I. A., Shalaby, A. A., Abdallah, H. M. L., El-Zohairy, N. F. & Bahr, H. I. Ameliorative effect of garden cress (*Lepidium sativum* L.) seeds ethanolic extract on high fat diet-prompted non-alcoholic fatty liver disease in the rat model: Impact on 3-hydroxy-3-methylglutaryl-coenzyme a reductase and vascular endothelial growth factor. *Adv. Anim. Vet. Sci.* **8**, 1–10. <https://doi.org/10.17582/journal.aavs/2020/8.s1.1.10> (2020).
57. Mohamed, H. S., Kholief, T., Mohamed, R. W. & Abd El-Rhman, A. The modulatory effects of black chia (*Salvia hispanica*) and garden cress (*Lepidium sativum*) seeds on Ne-CML formation in streptozotocin-injected rats. *J. Herbmed Pharmacol.* **12**, 250–261 (2023).
58. Abuelgasim, A. I., Nuha, H. S. & Mohammed, A. H. Hepatoprotective effect of *Lepidium sativum* against carbon tetrachloride induced damage in rats. *Res. J. Anim. Vet. Sci.* **3**, 20–23 (2008).
59. El-Akad, R. H., Ibrahim, F. M., Ashour, W. E., Abou Zeid, A. H. & Mohammed, R. S. Fruit metabolome profiling via HR-UPLC/MS and its in vitro antiarthritic activity. *S. Afr. J. Bot.* **151**, 649–654 (2022).
60. Adams, R. P. *Identification of Essential Oil Components by Gas Chromatography/Mass Spectrometry* 5th edn. (Texensis Publishing, 2017).
61. Sayed, D. F., Afifi, A. H., Temraz, A. & Ahmed, A. H. Metabolic profiling of *Mimusops elengi* Linn. leaves extract and in silico anti-inflammatory assessment targeting NLRP3 inflammasome. *Arab. J. Chem.* **16**(6), 104753 (2023).
62. Demiryilmaz, I. et al. Biochemically and histopathologically comparative review of thiamine's and thiamine pyrophosphate's oxidative stress effects generated with methotrexate in rat liver. *Med. Sci. Monit.* **18**, BR475–BR481. <https://doi.org/10.12659/msm.883591> (2012).
63. Yogesh Chand, Y., Srivastav, D. N. & Seth, A. K. Invivo antioxidant potential of *Lepidium sativum* L. seeds in albino rats using cisplatin induced nephrotoxicity. *Inter. J. Phytomed.* **2**, 292–298 (2010).
64. Livak, K. J. & Schmittgen, T. D. Analysis of relative gene expression data using real-time quantitative PCR and the 2(-Delta Delta C(T)) Method. *Methods* **25**, 402–408 (2001).
65. Drury, R. A. B. & Wallington, E. A. *Carleton's Histological Technique* 5th edn. (Oxford University Press, 1980).
66. Chen, Y. Y. et al. Intrahepatic macrophage populations in the pathophysiology of primary sclerosing cholangitis. *JHEP Rep.* **1**, 369–376 (2019).

Author contributions

A.I.E. and H.A.S. conceived of the presented idea and designed the manuscript plan, R.H.E. and A.H.A. performed the oil analysis and molecular docking, D.M.M. carried out the genetic analysis; H.A.S. & S.L.E. performed the histological analysis, A. I.E. and D.M.M. wrote the manuscript with input from all authors.

Funding

Open access funding provided by The Science, Technology & Innovation Funding Authority (STDF) in cooperation with The Egyptian Knowledge Bank (EKB).

Declarations

Competing interests

The authors declare no competing interests.

Ethics approval

The animal experiments were approved by the Ethics Committee of the National Research Centre (Approval

No. 09410125).

Additional information

Correspondence and requests for materials should be addressed to A.I.E.m.

Reprints and permissions information is available at www.nature.com/reprints.

Publisher's note Springer Nature remains neutral with regard to jurisdictional claims in published maps and institutional affiliations.

Open Access This article is licensed under a Creative Commons Attribution 4.0 International License, which permits use, sharing, adaptation, distribution and reproduction in any medium or format, as long as you give appropriate credit to the original author(s) and the source, provide a link to the Creative Commons licence, and indicate if changes were made. The images or other third party material in this article are included in the article's Creative Commons licence, unless indicated otherwise in a credit line to the material. If material is not included in the article's Creative Commons licence and your intended use is not permitted by statutory regulation or exceeds the permitted use, you will need to obtain permission directly from the copyright holder. To view a copy of this licence, visit <http://creativecommons.org/licenses/by/4.0/>.

© The Author(s) 2025